Benzenium Ion Chemistry on Solid Metal Halide Superacids: In Situ ^{13}C NMR Experiments and Theoretical Calculations

Teng Xu, Dewey H. Barich, Paul D. Torres, and James F. Haw*

Contribution from the Laboratory for Magnetic Resonance and Molecular Science, Department of Chemistry, Texas A&M University, College Station, Texas 77843

Received September 3, 1996[⊗]

Abstract: The benzenium, toluenium, and ethylbenzenium ions were synthesized on aluminum bromide by coadsorption of the precursors with either HBr or alkyl bromide. Principal components of the ^{13}C chemical shift tensors for the ring carbons of these species were measured from magic angle spinning spectra. The benzenium ion was static at 77 K but underwent both proton scrambling and anisotropic rotation at 298 K as well as oligomerization at higher loadings. The *para* form of the toluenium ion was the dominant isomer at 77 K, but a temperature-dependent equilibrium between the *para* and *ortho* isomers was observed at 273 K. Observations of $^{1}H-^{13}C$ self-decoupling and loading-dependent ^{13}C shifts for small amounts of toluene on high-purity $AlBr_3$ demonstrate the existence of trace Brønsted sites on an important Friedel−Crafts catalyst. Geometries of the benzenium ions were optimized with both MP2/6-311+G* and density functional calculations at B3LYP/6-311+G*; these were in very good agreement with one another. Energy calculations at MP4(fc,sdq)/6-311+G*//MP2/6-311+G* with thermal corrections resulted in good agreement between calculated and measured proton affinities for benzene, toluene, and ethylbenzene. For the toluenium ion, the energies of the *ortho* and *meta* isomers were 1.2 and 5.4 kcal/mol, respectively, above the *para* isomer, consistent with the temperature-dependent ^{13}C NMR spectra in the solid state. ^{13}C chemical shift tensors calculated at the GIAO-MP2/tzp/dz//MP2/6-311+G* and GIAO-MP2/tzp/dz//B3LYP/6-311+G* levels of theory were in very close agreement with each other and generally in satisfactory agreement with experimental principal components. The calculated tensors of benzenium ion were modified to account for the two dynamical processes described above, and a combination of these reproduced the experimental observation of a single, axially symmetric tensor at 298 K.

Introduction

Arenium ions[1] (e.g., benzenium **1**) have a long and distinguished history in organic chemistry, the first 60 or so years of which are described elsewhere.[2−5] These carbocations, formed by protonation or alkylation of aromatic rings (e.g., Scheme 1), are central to electrophilic aromatic substitutions or rearrangements in acidic solutions and the gas phase.

In the mid-to-late 1950s, Olah and Kuhn[6,7] isolated simple alkylbenzenium ions as their tetrafluoroborate salts. Baenziger and Nelson measured the structure of the tetrachloroaluminate salt of the heptamethylbenzenium ion.[8] The first solution ^{1}H NMR studies of alkyl-substituted benzenium ions were carried out more-or-less simultaneously by Doering et al.[9] and MacLean et al.[10] followed by Olah,[11] MacLean and Mackor,[12,13] and

Scheme 1

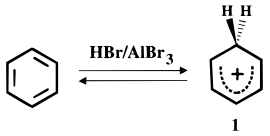

1

Gillespie.[14] This early work was greatly elaborated by Olah and co-workers,[15−19] who reported ^{1}H and ^{13}C NMR measurements in magic acid and related solution superacids. Mass spectrometry, ICR, and related methods[20−26] have been exten-

* Author to whom correspondence should be addressed.

[⊗] Abstract published in *Advance ACS Abstracts,* January 1, 1997.

(1) Arenium ions are also known as Pfeiffer−Wizinger complexes, Brown σ-complexes, Wheland intermediates, cyclohexadienyl ions, and arenonium ions. In this contribution, the nomenclature arenium ion is used throughout, reflecting the trivalent carbenium ion nature of these ions.

(2) Olah, G. A. *Friedel-Crafts and Related Reactions*; Wiley & Sons: New York, 1963; Vol. 1.

(3) Olah, G. A. *Friedel-Crafts Chemistry*; Wiley & Sons: New York, 1973.

(4) Brouwer, D. M.; Mackor, E. L.; MacLean, C. In *Carbonium Ions*; Olah, G. A., Schleyer, P. v. R., Eds.; Wiley Interscience: New York, 1970; pp 837−898.

(5) Farcasiu, D. *Acc. Chem. Res.* **1982**, *15*, 46−51.

(6) Olah, G.; Kuhn, S.; Pavlath, A. *Nature* **1956**, *178*, 693−694.

(7) Olah, G. A.; Kuhn, S. J. *J. Am. Chem. Soc.* **1958**, *80*, 6535−6539.

(8) Baenziger, N. C.; Nelson, A. D. *J. Am. Chem. Soc.* **1968**, *90*, 6602−6607.

(9) Doering, W. v. E.; Saunders, M.; Boyton, H. G.; Earhart, H. W.; Wadley, E. F.; Edwards, W. R.; Laber, G. *Tetrahedron* **1958**, *4*, 178−185.

(10) MacLean, C.; van der Waals, J. H.; Mackor, E. L. *Mol. Phys.* **1958**, *1*, 247−256.

(11) Olah, G. A. *J. Am. Chem. Soc.* **1965**, *87*, 1103−1108.

(12) MacLean, C.; Mackor, E. L. *Mol. Phys.* **1961**, *4*, 241−253.

(13) MacLean, C.; Mackor, E. L. *Discuss. Faraday Soc.* **1962**, *34*, 165−176.

(14) Birchall, T.; Gillespie, R. J. *Can. J. Chem.* **1964**, *42*, 502−513.

(15) Olah, G. A.; Schlosberg, R. H.; Porter, R. D.; Mo, Y. K.; Kelly, D. P.; Mateescu, G. D. *J. Am. Chem. Soc.* **1972**, *94*, 2034−2043.

(16) Olah, G. A.; Liang, G.; Westerman, P. *J. Am. Chem. Soc.* **1973**, *95*, 3698−3705.

(17) Olah, G. A.; Mateescu, G. D.; Mo, Y. K. *J. Am. Chem. Soc.* **1973**, *95*, 1805−1814.

(18) Olah, G. A.; Spear, R. J.; Messina, G.; Westerman, P. W. *J. Am. Chem. Soc.* **1975**, *97*, 4051−4055.

(19) Olah, G. A.; Staral, J. S.; Asencio, G.; Liang, G.; Forsyth, D. A.; Mateescu, G. D. *J. Am. Chem. Soc.* **1978**, *100*, 6299−6308.

(20) Freiser, B. S.; Woodin, R. L.; Beauchamp, J. L. *J. Am. Chem. Soc.* **1975**, *97*, 6893−6894.

(21) Kuck, D.; Ingeman, S.; de Koning, L. J.; Grutzmacher, H.-F.; Nibbering, N. M. *Angew. Chem., Int. Ed. Engl.* **1985**, *24*, 693−695.

(22) Holman, R. W.; Gross, M. L. *J. Am. Chem. Soc.* **1989**, *111*, 3560−3565.

(23) Attina, M.; Cacace, F.; Ricci, A. *J. Am. Chem. Soc.* **1991**, *113*, 5937−5942.

(24) Cacace, F.; Crestoni, M. E.; Fornarini, S. *J. Am. Chem. Soc.* **1992**, *114*, 6776−6784.

(25) Cacace, F.; Crestoni, M. E.; Fornarini, S.; Kuck, D. *J. Am. Chem. Soc.* **1993**, *115*, 1024−1031.

S0002-7863(96)03082-X CCC: $14.00

sively applied to characterize the rates and mechanisms of arenium ion reactions in the gas phase. Variable temperature NMR was applied by Farcasiu[27] and others[15] to identify *ortho*−*para* equilibria for alkylbenzenium ions in solution. Extension of solution ^{1}H NMR studies to aluminum halide acid systems was first reported by Doering et al.[9] and Koptyug et al.[28,29] Olah and co-workers reported the first ^{13}C NMR study of the "red oils" formed in Friedel−Crafts reactions.[18] Studies of aluminum halide molten salts are of current interest; these were originally formulated with *N*-1-butylpyridinium chloride (NPC) or 1-ethyl-3-methyl-1*H*-imidazolium chloride (EMIC) as in HCl/$AlCl_3$/EMIC,[30,31] but as shown recently by Ma et al.,[32] HBr/$AlBr_3$/TMSuBr (TMSuBr = trimethylsulfonium bromide) is a convenient molten salt system that can partially protonate benzene while leaving wide spectral windows.

Recently Sieber, Schleyer and Gauss[33] carried out MP2/6-31G* optimizations of **1** that confirmed its C_{2v} symmetry; furthermore they carried out correlated GIAO-MP2 ^{13}C chemical shift calculations and found excellent agreement between the calculated isotropic shifts and those measured previously in solution. There is now a body of literature that demonstrates the importance of properly including electron correlation in chemical shift calculations for carbenium ions and related species, especially those with multiple bonds.[33−36] A recently published GIAO-DFT (density functional theory) method that provides calculations of acceptable accuracy for many test cases was clearly less accurate than MP2 for the specific case of **1**.[37]

Beginning in 1989,[38] we have used variable temperature in situ magic angle spinning (MAS) NMR to study the chemistry of solid acids.[39] More recently, this work has been combined with theoretical calculations of the structures, energies, and chemical shifts for species proposed to exist on solid acids. In 1995, we studied H/D exchange reactions of benzene on HY zeolite and demonstrated that the reaction coordinate did not include a benzenium ion intermediate.[40] We also published (as a control experiment) the first NMR study in frozen magic acid; we observed the static benzenium ion at 83 K. Also in 1995, we reported the principal components of the ^{13}C chemical shift tensors of the *tert*-butyl and acetylium cations formed on $AlCl_3$.[41]

In the present paper we report the first detailed study of benzenium ions on solid acids. We prepared the benzenium, toluenium, and ethylbenzenium ions on $AlBr_3$ and/or HBr/$AlBr_3$. In situ ^{13}C MAS NMR was used to measure the principal components of the ^{13}C chemical shift tensors of the cations as well as to observe some of the dynamics of electrophilic aromatic substitution on metal halide solid acids. ^{13}C chemical shift tensors for benzenium ions, available for the first time, motivate a comparison of experimental and calculated values.

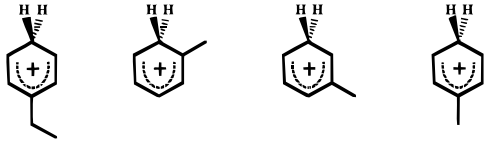

2 *o*-**3** *m*-**3** *p*-**3**

Geometries of the benzenium ion (**1**), *para*-protonated ethylbenzenium ion (**2**), and three isomers of the toluenium ion (*o*-**3**, *m*-**3**, and *p*-**3**) were determined at the MP2/6-311+G* level of theory and by density functional theory at B3LYP/6-311+G*.[42] The geometries obtained using DFT were very similar to those obtained with MP2. The calculated proton affinities (PAs) were in good agreement with experimental proton affinities for the precursors. ^{13}C chemical shift tensors were calculated at both GIAO-MP2/tzp/dz//MP2/6-311+G* and GIAO-MP2/tzp/dz//B3LYP/6-311+G*. These values were in satisfactory agreement with experiment, even without attempts to model the medium in the calculations.

Experimental Section

Materials. Anhydrous aluminum bromide (99.99%), hydrogen bromide (99%), bromomethane (99.5%), bromoethane (99%), benzene (99.9%), and toluene (99.8%) were purchased from Aldrich. Bromomethane-^{13}C, benzene-$^{13}C_6$, benzene-$^{13}C_1$, toluene-ring-$^{13}C_6$, and toluene-α-^{13}C were purchased from Isotec. ^{13}C enrichment in all the ^{13}C-labeled compounds is 99% or greater.

Sample Preparation for MAS NMR. All samples were prepared using a standard CAVERN device described previously.[43] Anhydrous $AlBr_3$ was ground to a fine powder inside a dry box under a nitrogen atmosphere; 0.6−0.8 g of $AlBr_3$ powder was loaded into a 7.5-mm NMR rotor and evacuated to a final pressure of less than 10^{-4} Torr in the CAVERN device. Adsorptions were done at subambient temperatures on a vacuum line. The uptake of benzene and toluene is strongly dependent upon the adsorption temperature; the optimum adsorption temperature was found to be ca. 243 K for benzene and ca. 273 K for toluene. The loading of the aromatics was typically 0.1−0.2 equiv (molecule/$AlBr_3$). Reactions between benzene and alkyl halides were usually carried out between 200 and 243 K to avoid the formation of di- or multisubstituted benzenium ions. Loadings of alkyl halides were slightly higher than those of benzene in order to achieve complete conversion to benzenium ions, as unreacted benzene interfered with measurement of the ^{13}C principal components of the benzenium ions.

A slightly different procedure was used to synthesize benzenium ions on HBr/$AlBr_3$. For example, benzene was adsorbed onto $AlBr_3$ at 243 K, and the sample was further cooled to 150 K and exposed to 600−700 Torr of HBr gas. The rotor was capped at 77 K and transferred to a precooled NMR probe.

NMR Spectroscopy. ^{13}C MAS NMR experiments were performed on a modified Chemagnetics CMX-300 MHz spectrometer operating at 75.36 MHz. Hexamethylbenzene (17.4 ppm for the methyl carbons) was used as the external chemical shift standard. Chemical shift parameters are reported relative to tetramethylsilane (TMS). Chemagnetics-style pencil probes spun 7.5-mm zirconia rotors with active spin speed control (±3 Hz). A number of NMR experiments were performed at different temperatures, including: cross-polarization[44] (CP, contact time = 1−2 ms, pulse delay = 1−4 s, 2000−4000 transients),

(26) Aschi, M.; Attina, M.; Cacace, F. *Angew. Chem., Int. Ed. Engl.* **1995**, *34*, 1589−1591.
(27) Farcasiu, D.; Melchor, M. T.; Craine, L. *Angew. Chem., Int. Ed. Engl.* **1977**, *16*, 315−317.
(28) Koptyug, V. A.; Rezvukhin, A. I.; Zaev, E. E.; Molin, Y. N. *Izv. Akad. Nauk SSSR* **1963**, 1700.
(29) Koptyug, V. A.; Rezvukhin, A. I.; Zaev, E. E.; Molin, Y. N. *Zh. Obshch. Khim.* **1964**, *34*, 3999−4002.
(30) O'Donnell, T. A. *Superacids and Acidic Melts as Inorganic Chemical Reaction Media*; VCH: New York, 1993.
(31) Wilkes, J. S.; Levisky, J. A.; Wilson, R. A.; Hussey, C. L. *Inorg. Chem.* **1982**, *21*, 1263−1264.
(32) Ma, M.; Johnson, K. E. *J. Am. Chem. Soc.* **1995**, *117*, 1508−1513.
(33) Sieber, S.; Schleyer, P. v. R.; Gauss, J. *J. Am. Chem. Soc.* **1993**, *115*, 6987−6988.
(34) Gauss, J. *J. Chem. Phys.* **1993**, *99*, 3629−3643.
(35) Gauss, J. *Chem. Phys. Lett.* **1994**, *229*, 198−203.
(36) Gauss, J.; Stanton, J. F. *J. Chem. Phys.* **1995**, *103*, 3561−3577.
(37) Cheeseman, J. R.; Trucks, G. W.; Keith, T. A.; Frisch, M. J. *J. Chem. Phys.* **1996**, *104*, 5497−5509.
(38) Haw, J. F.; Richardson, B. R.; Oshiro, I. S.; Lazo, N. L.; Speed, J. A. *J. Am. Chem. Soc.* **1989**, *111*, 2052−2058.
(39) Haw, J. F.; Nicholas, J. B.; Xu, T.; Beck, L. W.; Ferguson, D. B. *Acc. Chem. Res.* **1996**, *29*, 259−267.
(40) Beck, L. W.; Xu, T.; Nicholas, J. B.; Haw, J. F. *J. Am. Chem. Soc.* **1995**, *117*, 11594−11595.
(41) Xu, T.; Torres, P. D.; Beck, L. W.; Haw, J. F. *J. Am. Chem. Soc.* **1995**, *117*, 8027−8028.
(42) Becke, A. D. *Phys. Rev. A* **1988**, *38*, 3098−3100.
(43) Munson, E. J.; Ferguson, D. B.; Kheir, A. A.; Haw, J. F. *J. Catal.* **1992**, *136*, 504−509.
(44) Pines, A.; Gibby, M. G.; Waugh, J. S. *J. Chem. Phys.* **1973**, *59*, 569−590.

cross-polarization with interrupted decoupling[45] (contact time = 1−2 ms, pulse delay = 1−4 s, 2000−4000 transients, dipolar dephasing time of 50 μs), and single-pulse excitation (Bloch decay) with or without proton decoupling (pulse delay = 4−20 s, 200 transients).

Experiments were carried out and reported using both benzene-$^{13}C_1$ and benzene-$^{13}C_6$ as the label source for ring carbons. The principal components of the chemical shift tensors for the benzenium ions were measured by fitting the side band intensities of the ^{13}C CP MAS spectra using the Herzfeld−Berger algorithm.[46] For accurate measurements, several orders of spinning side bands are required for each isotropic peak; therefore, slow spinning speeds are appropriate. Typical spinning speeds were ca. 4.0 kHz, which is somewhat faster than the ^{13}C−^{13}C dipolar coupling between two adjacent ^{13}C nuclei in static benzene. The estimated uncertainties in the measured isotropic shifts are <1 ppm, while the indeterminate errors in the principal component measurements are larger (vide infra).

The isotropic shift (δ_{iso}) is the average of three principal components ($\delta_{11} \geq \delta_{22} \geq \delta_{33}$), i.e.,

$$\delta_{iso} = {}^1/_3(\delta_{11} + \delta_{22} + \delta_{33})$$

The asymmetry factor (η) and chemical shift anisotropy (CSA) are defined by the following equations to comform with the convention found in the compilation of principal component data by Duncan:[47]

$$\text{for } |\delta_{11} - \delta_{iso}| \geq |\delta_{33} - \delta_{iso}|,\ \text{CSA} = {}^3/_2(\delta_{11} - \delta_{iso}),\quad \eta = (\delta_{22} - \delta_{33})/(\delta_{11} - \delta_{iso})$$

$$\text{for } |\delta_{11} - \delta_{iso}| \leq |\delta_{33} - \delta_{iso}|,\ \text{CSA} = {}^3/_2(\delta_{33} - \delta_{iso}),\quad \eta = (\delta_{22} - \delta_{11})/(\delta_{33} - \delta_{iso})$$

Computations. We fully optimized the benzenium ions **1**−**3** using analytical gradient techniques within the program Gaussian 94.[48] All of the geometries reported here were obtained using the 6-311+G* basis set.[49] Electron correlation was treated using either second-order Møller−Plesset perturbation theory (MP2)[50] or density functional theory using the B3LYP[42] exchange functional. Core electrons were frozen in the MP2 optimizations and the MP4 energy calculations. We allowed the molecules complete flexibility during geometry optimizations at levels of theory below those reported. From those preliminary results, we imposed reasonable symmetry constraints on the final optimizations. For the final MP2 optimized geometries, we also performed single-point energy calculations at MP4(fc,sdq) and MP2 frequency calculations to obtain the zero-point energies.

In order to circumvent the problem of gauge dependence common to all magnetic properties, we used gauge including atomic orbitals (GIAOs)[51,52] in the chemical shift calculations. ^{13}C chemical shift tensors were calculated at the GIAO-MP2/tzp/dz[53] level of theory (hydrogens with the double-zeta polarized, dz, and carbons with the triple-zeta polarized, tzp, basis sets of Horn and Alhrichs).[54,55] Schleyer and co-workers have demonstrated that a similar scheme, combining optimizations at the MP2/6-31G* level with GIAO-MP2/tzp/dz NMR calculations, gives good agreement with experimental isotropic shifts for a variety of cations, especially **1**.[33]

We used the program ACES II for the GIAO-MP2 chemical shift calculations.[56] ^{13}C chemical shifts are reported relative to the value for tetramethylsilane (TMS) calculated at the same level of theory. For the basis sets employed here, the absolute ^{13}C shieldings of TMS were 199.0 (MP2 geometry) and 198.9 (B3LYP geometry).

Because the antisymmetric portion of the calculated tensor is generally not observed experimentally, the calculated tensors must be corrected prior to comparison with experiment. Thus, we first averaged the upper and lower triangles of the tensors and then diagonalized the symmetrized tensors. A program to easily take chemical shift tensor data from quantum chemistry codes, calculate principal components, and create data for plotting of the molecules and tensor orientations is available from the authors upon request.[57]

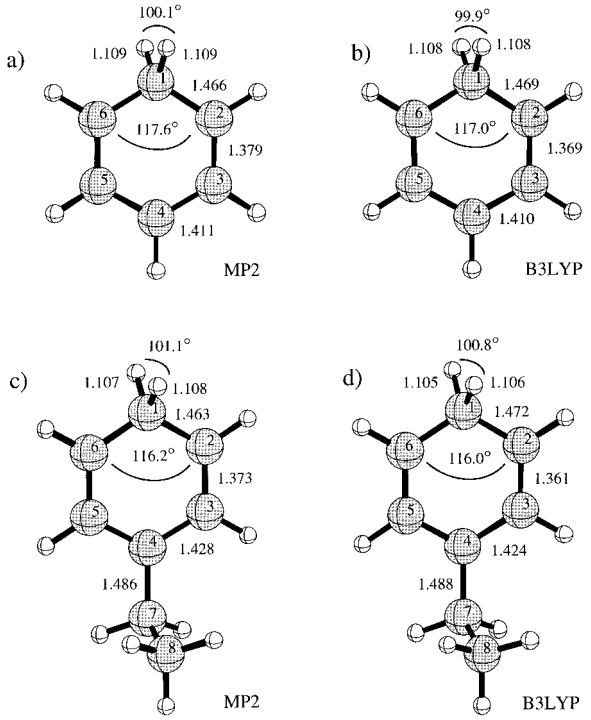

Figure 1. Calculated geometries of **1** and **2** with the selected bond distances (Å) and angles (deg) shown. Both MP2/6-311+G* and B3LYP/MP2/6-311+G* optimizations are shown. The geometries for **1** are in C_{2v} symmetry, and those for **2** are in C_s. The structures are slightly tilted about their C_1−C_4 axes to clarify the protonation of C_1.

Results

Geometries and Energies. Figure 1 presents and compares the geometries of **1** and **2** optimized at the MP2/6-311+G* and B3LYP/6-311+G* levels of theory. Discrepancies in bond distances between MP2 and DFT are no greater than 0.01 Å and are typically much less; the angles agree to within 0.6°. Our geometries for **1** are also in very close agreement with those reported by Schleyer and co-workers at MP2/6-31G*.[33] Figure 2 reports MP2/6-311+G* geometries for all three isomers of **3** as well as the B3LYP geometry for *p*-**3**. Again, the agreement between MP2 and DFT is satisfying.

Energies of **1**−**3** as well as their nonprotonated precursors were determined at the MP2/6-311+G* level of theory, further refined by calculating the zero-point and vibrational contributions as well as the single-point energies at MP4(fc,sdq). The

(45) Opella, S. J. *J. Am. Chem. Soc.* **1979**, *101*, 5854−5856.
(46) Herzfeld, J.; Berger, A. E. *J. Chem. Phys.* **1980**, *73*, 6021−6030.
(47) Duncan, T. M. *A Compilation of Chemical Shift Anisotropies*; Farragut Press: Chicago, IL, 1990.
(48) Frisch, M. J.; Trucks, G. W.; Schlegel, H. B.; Gill, P. M. W.; Johnson, B. G.; Robb, M. A.; Cheeseman, J. R.; Keith, T.; Petersson, G. A.; Montgomery, J. A.; Raghavachari, K.; Al-Laham, M. A.; Zakrzewski, V. G.; Ortiz, J. V.; Foresman, J. B.; Cioslowski, J.; Stefanov, B. B.; Nanayakkara, A.; Challacombe, M.; Peng, C. Y.; Ayala, P. Y.; Chen, W.; Wong, M. W.; Andres, J. L.; Replogle, E. S.; Gomperts, R.; Martin, R. L.; Fox, D. J.; Binkley, J. S.; Defrees, D. J.; Baker, J.; Stewart, J. P.; Head-Gordon, M.; Gonzalez, C.; Pople, J. A. Gaussian 94, Revision B.1. Gaussian Inc.: Pittsburgh, PA, 1995.
(49) Hehre, W. J.; Radom, L.; Schleyer, P. v. R.; Pople, J. A. *Ab Initio Molecular Orbital Theory*; John Wiley & Sons: New York, 1986.
(50) Møller, C.; Plesset, M. S. *Phys. Rev.* **1934**, *46*, 618−622.
(51) Wolinski, K.; Hinton, J. F.; Pulay, P. *J. Am. Chem. Soc.* **1990**, *112*, 8251−8260.
(52) Ditchfield, R. *Mol. Phys.* **1974**, *27*, 789−807.
(53) Gauss, J. *Chem. Phys. Lett.* **1992**, *191*, 614−620.
(54) Schafer, A.; Horn, H.; Ahlrichs, R. *J. Chem. Phys.* **1992**, *97*, 2571−2577.
(55) Schafer, A.; Huber, C.; Ahlrichs, R. *J. Chem. Phys.* **1992**, *100*, 5829−5835.
(56) Stanton, J. F.; Gauss, J.; Watts, J. D.; Lauderdale, W. J.; Bartlett, R. J. ACES II, an ab initio quantum chemical program system.
(57) The program is available from the authors.

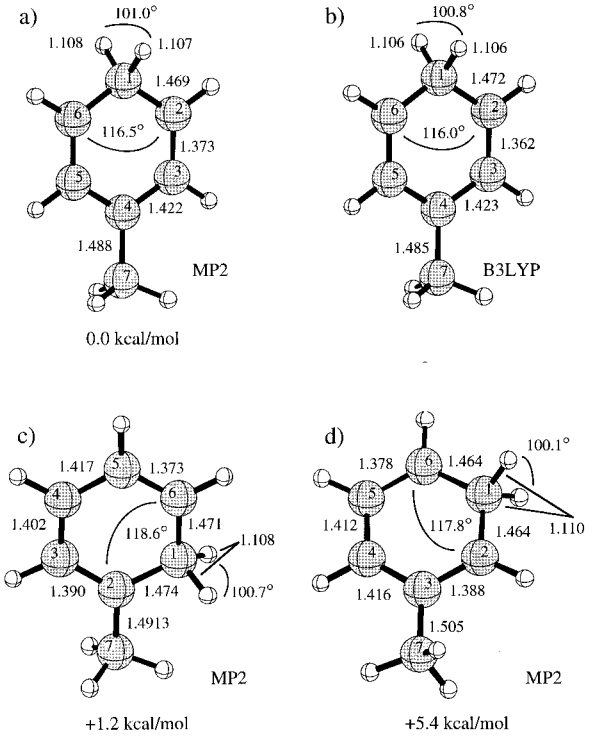

Figure 2. Calculated geometries of toluenium ions *o*-**3**, *m*-**3**, and *p*-**3** with the selected bond distances (Å) and angles (deg) shown. Reported geometries are in C_s symmetry. For parts a, c, and d, the total energy (kcal/mol) relative to part a is shown. MP2/6-311+G* geometries are shown for all isomers, and the B3LYP/6-311+G* geometry is also shown for *p*-**3**. The structures are again slightly tilted about their C_1-C_4 axes for clarity.

differences between the energies determined as MP4(fc,sdq)/6-311+G*//MP2/6-311+G* + ZPE (zero point energy) + vibration + translation + rotation for the benzenium ions and their precursors (Table 1) are in good agreement with experimental proton affinities, where available.[58] Comparison of the theoretical PAs for toluene protonation at the *ortho*, *meta*, and *para* positions evokes the well-known selectivity for Friedel−Crafts reactions carried out at low temperatures under thermodynamic control. Furthermore, the relative energies of *o*-**3**, *m*-**3**, and *p*-**3** suggest that temperature-dependent NMR studies should find *p*-**3** predominating at low temperatures and an *o*-**3**, *p*-**3** equilibrium at higher temperatures. Similar results were previously obtained by Farcasiu for ethylbenzene in superacid solution.[27]

NMR Experiments. The benzenium ion (**1**) was formed in 100% yield by protonation of benzene with excess HBr/$AlBr_3$, consistent with the findings of Farcasiu and co-workers.[59] Figure 3 motivates our selections of labeling ($^{13}C_6$ vs $^{13}C_1$) and loading for chemical shift principal component measurements and dynamic studies. The benzenium ion is static on the NMR time scale at 77 K, and spinning side band patterns are evident for all carbons. Comparison of spectra for **1** prepared from benzene-$^{13}C_6$ (Figure 3a) with that from benzene-$^{13}C_1$ (Figure 3b) shows that although the signal-to-noise ratio is superior with higher label content, even with a smaller number of scans, homonuclear dipolar coupling results in modest line broadening in Figure 3a. Although apparent ^{13}C principal components can be obtained from the side band amplitudes in Figure 3a, these intensities will be slightly altered by $^{13}C-^{13}C$ dipolar couplings; therefore, we report below ^{13}C shift data measured from singly-labeled aromatic rings, where possible, and exploit the higher signal-to-noise ratio available with fully ring-labeled cations in qualitative or semiquantitative studies of dynamics. The loading of benzene was ca. 0.1 equiv for the samples reported in Figure 3a,b; Figure 3c,d demonstrates the complications of trying to increase the signal-to-noise ratio by recourse to a higher benzene loading, 0.25 equiv. At 77 K, both **1** and unreacted benzene-$^{13}C_1$ are present, and upon heating to 298 K, the spectrum (Figure 3d) strongly suggests oligomeric (i.e., phenyl-substituted) benzenium ions.

In the following studies, the benzene loadings were low enough that neither unreacted benzene nor oligomeric products were complicating factors, and we were able to measure the isotropic shifts and principal components. The experimental and theoretical shift values are reported in Table 2. Experimental shift components reported for C_2 through C_6 were obtained from experiments using benzene-$^{13}C_1$, but the small side band intensities for sp^3 carbon C_1 required that its components be estimated from experiments employing benzene-$^{13}C_6$. The 95% confidence intervals on the experimental data reported in Table 2 are the result of four measurements.

Figure 4 reports a detailed study of the dynamics of **1**. At 193 K and higher the rigid-lattice spectrum collapses to a single isotropic peak and associated side bands as a result of proton exchange and other dynamics. Bloch decay spectra at 298 K show that some of the benzenium ions undergo isotropic motion, while the remainder exhibit anisotropic motion; the latter component was isolated in a cross-polarization spectrum, and Herzfeld−Berger analysis of the side band intensities revealed near-axial symmetry for the chemical shift tensor ($\delta_{11} = 208$ ppm, $\delta_{22} = 206$ ppm, and $\delta_{33} = 28$ ppm).

Alkylbenzenium ions were prepared either by protonation of the corresponding alkylbenzenes or by alkylation of benzene. We prepared **2** by reacting benzene on $AlBr_3$ with an excess of bromoethane (natural abundance) at 243 K. The experimental spectrum in Figure 5a was acquired at 77 K. As was the case for all of the ions studied here, for any selection of spinning speed there was at least modest overlap for some of the side bands. We acquired a spectrum with modest overlap and decomposed each overlapped feature with a line-fitting program. We further refined the resulting individual intensities using a nonlinear least-squares algorithm to obtain a best fit of the original spectrum; Figure 5b,c shows the optimized and difference spectra, respectively. The decomposed peak amplitudes from Figure 4b were then used in the Herzfeld−Berger analysis. Experimental and theoretical chemical shift data are reported in Table 3 for ion **2**. As demonstrated by Farcasiu,[27] the solution spectrum of **2** varies with temperature as a result of the temperature dependence of the *para*−*ortho* equilibrium. We qualitatively observed this effect in the solid state, but further reactions of ion **2** to yield various degrees of substitution occurred at higher temperatures, and we did not further characterize the dynamics of **2**.

We prepared the toluenium ion **3** by the reaction of a stoichiometric amount of bromomethane and benzene on $AlBr_3$ at 233 K. The ^{13}C principal components of the *para* isomer *p*-**3** were measured from a sample prepared by reacting bromomethane and benzene-$^{13}C_1$ (Table 4). Like ion **1**, *p*-**3** was sufficiently mobile at higher temperatures that motional averaging eliminated the side bands. In addition, the resonances of C_1 (49 ppm) and $C_{3,5}$ (139 ppm) were noticeably broadened at 213 K (Figure 6) and broadened almost beyond detection at 243 K. At 273 K, two slightly broadened peaks were clearly resolved at 73 and 128 ppm, which were the population-

(58) Meot-Ner, M.; Sieck, L. W. *J. Am. Chem. Soc.* **1991**, *113*, 4448−4460.

(59) Farcasiu, D.; Fisk, S. L.; Melchior, M. T.; Rose, K. D. *J. Org. Chem.* **1982**, *47*, 453−457.

Table 1. Theoretical Gas Phase Energies and Proton Affinities of the Benzenium Ions[a]

molecule	MP2(fc) (Hartrees)	MP4(fc,sdq) (Hartrees)	ZPE (Hartrees)	vibrational (Hartrees)	PA (kcal/mol)	exptl PA[b] (kcal/mol)
benzene	−231.540 480	−231.572 401	0.097 778	0.004 505		
1	−231.824 142	−231.867 871	0.110 021	0.005 445	178.6	181.3
toluene	−270.726 070	−270.768 016	0.125 841	0.006 260		
p-**3**	−271.022 033	−271.077 373	0.138 204	0.007 002	187.4	189.8
o-**3**	−271.019 907	−271.074 369	0.137 800	0.006 364	186.2	
m-**3**	−271.014 547	−271.067 628	0.137 568	0.006 526	182.0	
ethylbenzene	−309.908 321	−309.960 759	0.155 926	0.007 834		
2	−310.205 883	−310.271 747	0.167 785	0.008 207	189.0	191.6

[a] MP2(fc) energies are from the MP2 optimizations. MP4(fc,sdq) single-point energies were calculated for the MP2 optimized structures. Thermal contributions (zero-point energies (ZPE) and vibrational corrections) were determined for the MP2 geometries at 298.15 K and 1 atm. Proton affinities (PA) are reported as $-\Delta H$ for the formation of HB^+ from B and H^+. Thus, the total enthalpy (not shown) is determined as MP4(fc,sdq)/6-311+G*//MP2/6-311+G* + ZPE + vib + trans + rot. Finally, $\Delta H = H_{BH^+} - H_B - H_{H^+} + \Delta nRT = H_{BH^+} - H_B - {}^3/_2RT - RT = H_{BH^+} - H_B - {}^5/_2RT$. [b] The experimental proton affinity data were taken from Pedley, J. B. *Thermochemical Data of Organic Compounds*, 2nd ed.; Chapman & Hall: New York, 1986.

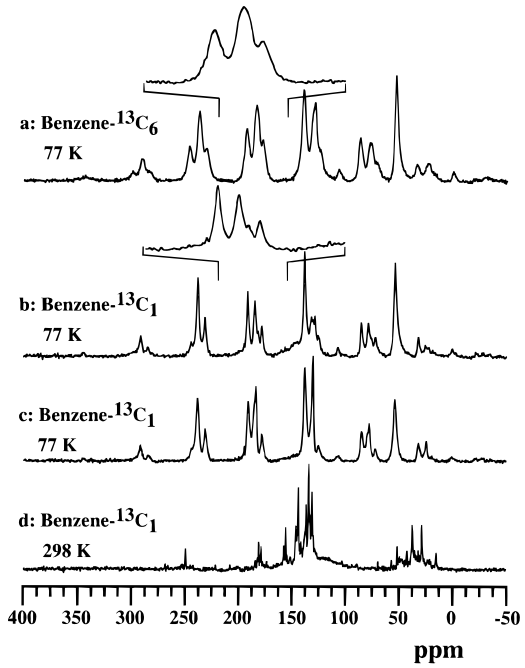

Figure 3. ^{13}C MAS (75.36 MHz) spectra of the benzenium ion prepared by the protonation of benzene-$^{13}C_6$ (spectrum a) or benzene-$^{13}C_1$ (spectra b−d) with $HBr/AlBr_3$. The loading of benzene was ca. 0.1 equiv for a and b and ca. 0.25 equiv for c and d. Spectra a−c are cross-polarization spectra acquired using 1 ms contact time and 2 s pulse delay; spectrum d is a Bloch decay spectrum with 4 s pulse delay. The higher loading of benzene results in oligomeric cations at room temperature. The spinning speeds and number of scans are (a) 4000 Hz, 2000 scans; (b) 4000 Hz, 3200 scans; (c) 4000 Hz, 2000 scans; (d) 2500 Hz, 100 scans.

weighted averages of the respective C_1 and $C_{3,5}$ shifts of the *para*- and *ortho*-protonated toluenium ions. Figure 6 shows a dramatic example of temperature-dependent isomerization of a carbocation on a solid acid and underscores the value of NMR measurements over a range of temperatures in studies of solid acid chemistry.

It is well known that olefins undergo Friedel−Crafts chemistry on $AlCl_3$ or $AlBr_3$, and it is assumed that there must be a trace of Brønsted acidity even on highly purified aluminum halide powders.[2] Figure 7 reports ^{13}C NMR results from a persuasive, if indirect, test of Brønsted acidity. We adsorbed very low loadings (ca. 0.01 equiv) of either toluene-α-^{13}C or toluene-ring-$^{13}C_6$ onto $AlBr_3$. At 298 K, the mobility of both toluene and **3** is such that $^1J_{^1H-^{13}C}$ scalar couplings can be measured for the methyl carbon. Figure 7a,b shows this very clearly; a well-resolved quartet ($^1J_{^1H-^{13}C} = 128$ Hz) is seen in the ^{13}C MAS NMR spectrum without ^1H decoupling. In contrast, the ring carbons show little if any evidence of $^1H-^{13}C$ scalar coupling, and they show modest but clear downfield shifts relative to toluene (Figure 7c,d). The magnitude of these downfield shifts is related to the ratio of accessible Brønsted sites to adsorbate molecules as seen when HBr is coadsorbed (Figure 7e).

Chemical Shift Calculations. In Tables 2−4 we report the principal components of the ^{13}C NMR shifts calculated at GIAO-MP2/tzp/dz on both the MP2 and DFT geometries and compare these with the experimental values for **1**, **2**, and *p*-**3**, respectively. For the isotropic shifts, the average absolute deviation between calculations and experiment is only 2 ppm (on the MP2 geometries), and the deviations in the principal components sometimes lie outside of the 95% confidence intervals for the measured quantities. Results obtained from a similar comparison using the shifts calculated from the DFT geometries are no worse, demonstrating that the B3LYP geometries are equally useful in the determination of the GIAO-MP2 chemical shifts. Note that the theoretical values for *p*-**3** are in close agreement with the low-temperature measurements of **3**, while the higher temperature experiments are consistent with fast exchange in a mixture of *p*-**3** and *o*-**3**.

Experimental measurement of the orientation of the principal axis systems in the molecular frame requires goniometer measurements on a large single crystal,[60−62] and such are unlikely for salts of benzenium ions; however, orientations are obtainable from theoretical tensors, and these are shown for **1**, *o*-**3**, *m*-**3**, and *p*-**3** in Figure 8.

Discussion

Benzenium Ion Dynamics on Solid Acids. Two types of dynamics are central to the experimental observations in this study: proton exchange and motional averaging of the benzenium ions (Scheme 2). The dynamics of **1** can be interpreted by comparison of Figure 4 with the theoretical tensors. **1** has four non equivalent tensors (Table 2 and Figure 4) at 77 K and a single, axially symmetric tensor at higher temperatures. We consider each of the dynamical processes first independently and then in combination. ^1H scrambling (Scheme 2a) alone results in a single tensor (as observed), but correct averaging of the six chemical shift tensors for this process results in $\delta_{11} = 246$ ppm, $\delta_{22} = 185$ ppm, and $\delta_{33} = 11$ ppm. These values are clearly inconsistent with experiment. At 298 K, some of

(60) Pausak, S.; Pines, A.; Waugh, J. S. *J. Chem. Phys.* **1973**, *59*, 591−595.
(61) Facelli, J. C.; Grant, D. M.; Michl, J. *Acc. Chem. Res.* **1987**, *20*, 152−158.
(62) Iuliucci, R. J.; Facelli, J. C.; Alderman, D. W.; Grant, D. M. *J. Am. Chem. Soc.* **1995**, *117*, 2336−2343.

Table 2. Calculated (GIAO) and Experimental[a] ^{13}C Chemical Shift Data for the Benzenium Cation **1**

level of theory[b]	carbon	δ_{iso} (ppm)	CSA (ppm)	η	δ_{11} (ppm)	δ_{22} (ppm)	δ_{33} (ppm)
MP2//MP2	1	53	82	0.74	108	46	5
MP2//B3LYP	1	52	83	0.72	108	45	5
exptl/C_6 (77 K)	1	53	84	0.45	109	37	12
MP2//MP2	2, 6	186	−258	0.56	320	223	14
MP2//B3LYP	2, 6	185	−257	0.55	318	223	13
exptl/C_1 (77 K)	2, 6	185	−251	0.44	305(11)	232(17)	18(11)
MP2//MP2	3, 5	142	−198	0.69	254	163	11
MP2//B3LYP	3, 5	141	−196	0.69	251	161	10
exptl/C_1 (77 K)	3, 5	138	−185	0.37	222(5)	177(5)	15(8)
MP2//MP2	4	177	−246	0.36	289	229	13
MP2//B3LYP	4	177	−248	0.35	289	231	12
exptl/C_1 (77 K)	4	178	−242	0.34	286(16)	231(27)	17(14)
exptl/C_6 (298 K)	all[c]	147	−179	0.02	208	206	28

[a] Isotropic chemical shifts and principal components are reported relative to TMS. The GIAO method was used for all chemical shift calculations. Numbers in parentheses adjacent to experimental principal components report the 95% confidence limits; for example, 305(11) means 305 ± 11 ppm. The same notation is used in Tables 3 and 4. [b] For brevity, the shorthand MP2//MP2 is used in the table to indicate MP2/tzp/dz NMR calculations on a geometry optimized using MP2/6-311+G*. Likewise, MP2//B3LYP indicates MP2/tzp/dz NMR of an optimization using B3LYP/6-311+G*. The precise notation for these calculations is MP2/tzp/dz//MP2/6-311+G* and MP2/tzp/dz//B3LYP/6-311+G*, respectively. [c] Rapid proton exchange makes all six carbons equivalent at this temperature.

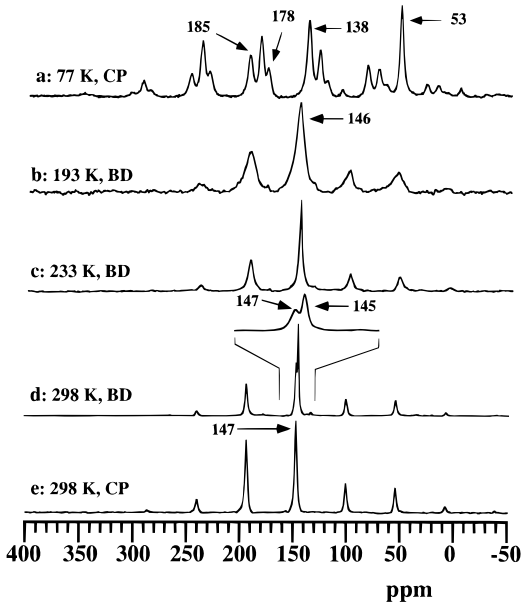

Figure 4. ^{13}C MAS spectra (75.36 MHz) showing the dynamics of the benzenium ion. The ion was prepared by reacting benzene-$^{13}C_6$ with HBr on $AlBr_3$ at 243 K; the loading of benzene-$^{13}C_6$ was less than 0.1 equiv: (a) cross-polarization (CP) spectrum of a static benzenium ion with four isotropic shifts; (b and c) Bloch decay (BD) spectra of the benzenium ion at 193 and 233 K, respectively; (d) Bloch decay spectrum of the benzenium ion at 298 K, showing two peaks at 147 and 145 ppm as can be seen in the inset; (e) cross-polarization spectrum of the benzenium ion at 298 K, showing the 147 ppm resonance and its associated side bands. The spinning speed was 4150 Hz for spectrum a and 3000 Hz for all other spectra.

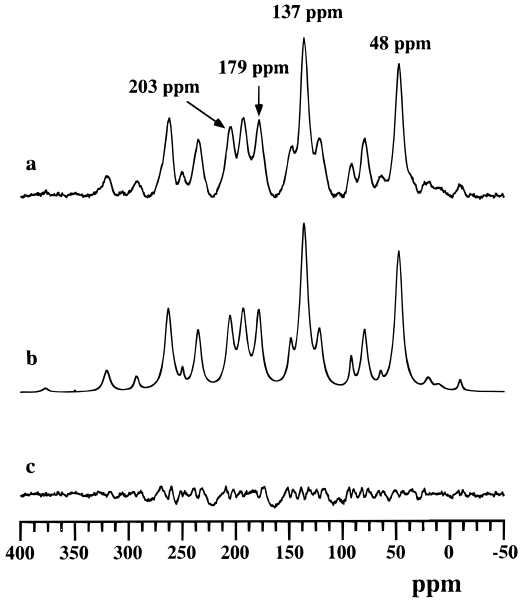

Figure 5. (a) ^{13}C CP/MAS spectrum (75.36 MHz) of the ethylbenzenium (ring-labeled) ion acquired at 77 K. The ion was prepared by reacting benzene-$^{13}C_6$ (less than 0.1 equiv) with excess bromoethane on $AlBr_3$ at 243 K. (b) Optimized simulated spectrum with Lorentzian line shapes using a nonlinear least-squares algorithm (see text). (c) Difference spectrum of a and b.

the benzenium ions in the experiment reported in Figure 4 undergo isotropic motion, but most undergo anisotropic motion (cf. Figure 4d,e). The observation of a single isotropic signal rules out rotation as the sole dynamical process. Consider the effect of proton exchange and isotropic rotation; in this case a single isotropic shift is predicted near 148 ppm. Instead consider both proton exchange and anisotropic rotation about an axis perpendicular to the plane defined by the ring (Scheme 2b). For this case, appropriate averaging of the tensors for **1** results in a single, axially symmetric tensor with $\delta_\perp = 216$ ppm (cf. 208 and 206 ppm exptl) and $\delta_{//} = 11$ ppm (cf. 28 ppm exptl). The agreement between experimental values and those derived from the latter model is very persuasive.

Dynamics were also observed for **2** and **3**, but these were more complicated. For the well-studied case of **3**, proton exchange is coupled with rotational averaging about multiple axes. Furthermore, the nonequivalence of the energies and sites in *o*-, *m*-, and *p*-**3** results in temperature-dependent equilibria and the characteristic appearance of the spectra in Figure 6.

Finally, the dynamics of proton exchange were also manifested in self-decoupling and loading-dependent chemical shifts for toluene on nominally pure $AlBr_3$ (Figure 7). Self-decoupling reveals low concentrations of Brønsted sites provided they are strong enough to protonate the adsorbate.

^{13}C Chemical Shift Tensors. This study advances the understanding of chemical shift tensors of carbocations. The claim of Sieber, Schleyer, and Gauss[33] that the GIAO-MP2/tzp/dz method produces reliable ^{13}C isotropic shifts for benzenium ions has been extended to include the principal components.

The orientations of the shift tensors are in accord with what one would expect from molecular symmetry and qualitative

Table 3. Calculated and Experimental ^{13}C Chemical Shift Data for the Ethylbenzenium Cation **2**

level of theory[b]	carbon	δ_{iso} (ppm)	CSA (ppm)	η	δ_{11} (ppm)	δ_{22} (ppm)	δ_{33} (ppm)
MP2//MP2	1	48	74	0.72	97	41	6
MP2//B3LYP	1	48	73	0.72	97	42	6
Exptl/C_6 (77 K)	1	48	74	0.71	97	41	6
MP2//MP2	2, 6	178	−242	0.58	305	212	16
MP2//B3LYP	2, 6	177	−241	0.58	305	211	17
exptl/C_1 (77 K)	2, 6	179	−239	0.38	289(9)	228(11)	20(4)
MP2//MP2	3, 5	143	−173	0.85	249	151	27
MP2//B3LYP	3, 5	141	−173	0.83	246	151	26
exptl/C_1 (77 K)	3, 5	137	−159	0.57	220	160	31
MP2//MP2	4	211	−286	0.21	326	286	20
MP2//B3LYP	4	211	−286	0.20	325	287	20
exptl/C_1 (77 K)	4	203	−276	0.05	301(8)	291(13)	19(6)
MP2//MP2	7	42	−32	0.74	61	45	21
MP2//MP2	7	42	−32	0.82	62	44	20
MP2//MP2	8	20	−29	0.16	32	29	1
MP2//MP2	8	21	−29	0.11	32	30	1

[a] Isotropic chemical shifts and principal components are reported relative to TMS. The GIAO method was used for all chemical shift calculations. [b] For brevity, the shorthand MP2//MP2 is used in the table to indicate MP2/tzp/dz NMR calculations on a geometry optimized using MP2/6-311+G*. Likewise, MP2//B3LYP indicates MP2/tzp/dz NMR of an optimization using B3LYP/6-311+G*. The precise notation for these calculations is MP2/tzp/dz//MP2/6-311+G* and MP2/tzp/dz//B3LYP/6-311+G*, respectively.

Table 4. Calculated ^{13}C chemical shift data for the *p*-, *o*-, and *m*-Toluenium Cations

level of theory[b]	carbon	δ_{iso} (ppm)	CSA (ppm)	η	δ_{11} (ppm)	δ_{22} (ppm)	δ_{33} (ppm)
			p-**3**				
MP2//MP2	1	49	74	0.76	98	43	5
MP2//B3LYP	1	48	74	0.74	98	42	5
Exptl/C_1 (77 K)	1	49	68	1.00	94	50	5
MP2//MP2	2, 6	179	−243	0.59	308	212	17
MP2//B3LYP	2, 6	178	−242	0.59	306	211	16
exptl/C_1 (77 K)	2, 6	179	−239	0.46	295(8)	222(7)	20(4)
MP2//MP2	3, 5	143	−174	0.83	250	153	27
MP2//B3LYP	3, 5	142	−173	0.83	247	152	26
exptl/C_1 (77 K)	3, 5	139	−164	0.65	229(3)	158(5)	30(5)
MP2//MP2	4	203	−278	0.07	302	289	18
MP2//B3LYP	4	204	−280	0.08	305	291	18
exptl/C_1 (77 K)	4	200	−287	0.10	305(19)	285(24)	9(11)
MP2//MP2	7	32	−40	0.21	48	42	5
MP2//B3LYP	7	32	−40	0.24	48	42	5
			o-**3**				
MP2//MP2	1	56	76	0.32	107	39	22
MP2//MP2	2	213	−289	0.19	327	291	20
MP2//MP2	3	143	−180	0.77	249	157	22
MP2//MP2	4	172	−234	0.39	280	219	16
MP2//MP2	5	139	−193	0.70	249	158	10
MP2//MP2	6	178	−240	0.59	305	211	18
MP2//MP2	7	30	−40	0.43	49	37	3
			m-**3**				
MP2//MP2	1	53	82	0.67	108	44	7
MP2//MP2	2	186	−241	0.58	313	220	25
MP2//MP2	3	157	−212	0.39	255	200	16
MP2//MP2	4	177	−220	0.44	283	218	30
MP2//MP2	5	142	−193	0.72	253	160	14
MP2//MP2	6	181	−253	0.57	314	217	13
MP2//MP2	7	22	−39	0.43	41	30	−4

[a] Isotropic chemical shifts and principal components are reported relative to TMS. The GIAO method was used for all chemical shift calculations. Experimental values are also reported for *p*-**3**. [b] For brevity, the shorthand MP2//MP2 is used in the table to indicate MP2/tzp/dz NMR calculations on a geometry optimized using MP2/6-311+G*. Likewise, MP2//B3LYP indicates MP2/tzp/dz NMR of an optimization using B3LYP/6-311+G*. The precise notation for these calculations is MP2/tzp/dz//MP2/6-311+G* and MP2/tzp/dz//B3LYP/6-311+G*, respectively.

ideas of ring currents. Consider cation **1** (Figure 8), which is of C_{2v} symmetry. The two planes of symmetry contained in this point group exactly specify the orientations of two of the tensor components, and the third is specified by orthogonality. The component perpendicular to the plane containing all ring carbons (the ring plane) is δ_{33}, the most shielded component. The component perpendicular to the second mirror plane is δ_{22}, and the least shielded direction δ_{11} is coincident with the C−H bond vectors. Since the δ_{22} component lies closest to the C−C bond vectors, it is more sensitive to determinate errors due to dipolar couplings. The apparent principal component data measured for the samples of **1** prepared from benzene-$^{13}C_6$ (not shown) had larger errors in δ_{22} than did the measurements based on benzene-$^{13}C_1$. All three isomers of **3** are of C_s symmetry. For *o*-**3** and *m*-**3**, the mirror plane contains all seven carbons (the ring plane). Such symmetry necessitates that two of the principal components lie in the ring plane perpendicular to one another, while the third is normal to that plane. In the *p*-**3** case the mirror plane contains atoms C_1, C_4, and C_7 and both protons bonded to C_1. While C_1, C_2, C_4, and C_6 all have δ_{33} components

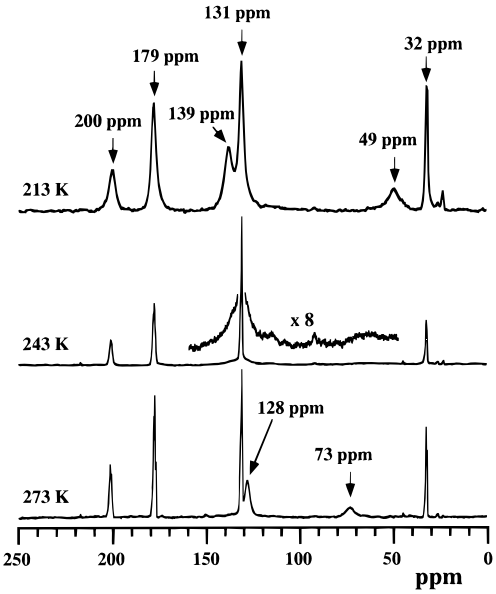

Figure 6. ^{13}C Bloch decay MAS spectra (75.36 MHz) showing the dynamics of the toluenium ion. The cation was synthesized by reacting bromomethane-^{13}C with benzene-$^{13}C_6$ on $AlBr_3$ at 233 K. The spectrum at 213 K shows the peaks for the toluenium ion at 32 (methyl), 49 (C_1), 179 (C_2), 139 (C_3), and 200 (C_4) ppm. The peak at 131 ppm is unreacted benzene-$^{13}C_6$. At 243 K, the peaks were much sharper, and the 139 and 49 ppm peaks were severely broadened. At 273 K, the spectrum shows two peaks at 128 and 73 ppm reflecting fast exchange between *o*-**3** and *p*-**3**.

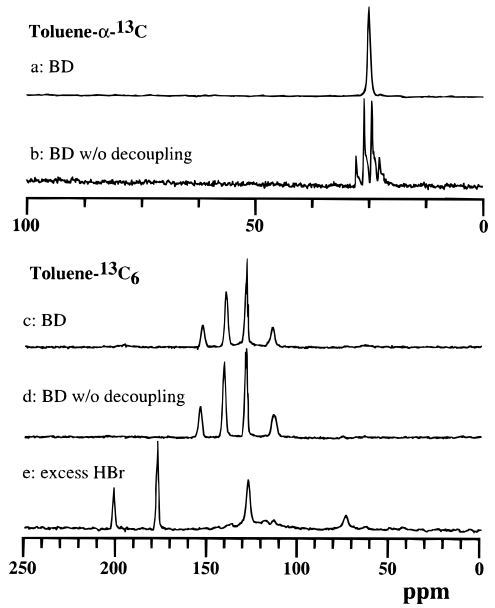

Figure 7. ^{13}C MAS spectra (75.36 MHz) of toluene on $AlBr_3$. Spectra (a−d) were acquired on samples in which toluene was adsorbed onto as-received $AlBr_3$, while spectrum e was acquired on a sample loaded with excess HBr. Toluene loadings for all the samples were ca. 0.01 equiv: (a) Bloch decay spectrum of toluene-α-^{13}C with proton decoupling; (b) Bloch decay spectrum of toluene-α-^{13}C without proton decoupling showing a quartet structure because of $^1J_{H-^{13}C}$ scalar coupling; (c) Bloch decay spectrum of toluene-ring-$^{13}C_6$ with proton decoupling showing four isotropic shifts, which are the weighted averages of the chemical shifts of a toluene and a toluenium ion; (d) Bloch decay spectrum of toluene-ring-$^{13}C_6$ without proton decoupling showing no ^{1}H−^{13}C scalar coupling; (e) Bloch decay spectrum of a toluene-ring-$^{13}C_6$ sample on $AlBr_3$ loaded with excess HBr, showing the formation of the toluenium ion.

perpendicular to the ring plane (δ_{11} and δ_{22} lie in the ring plane), the δ_{33} values for carbons C_3 and C_5 are tilted less than 1° from

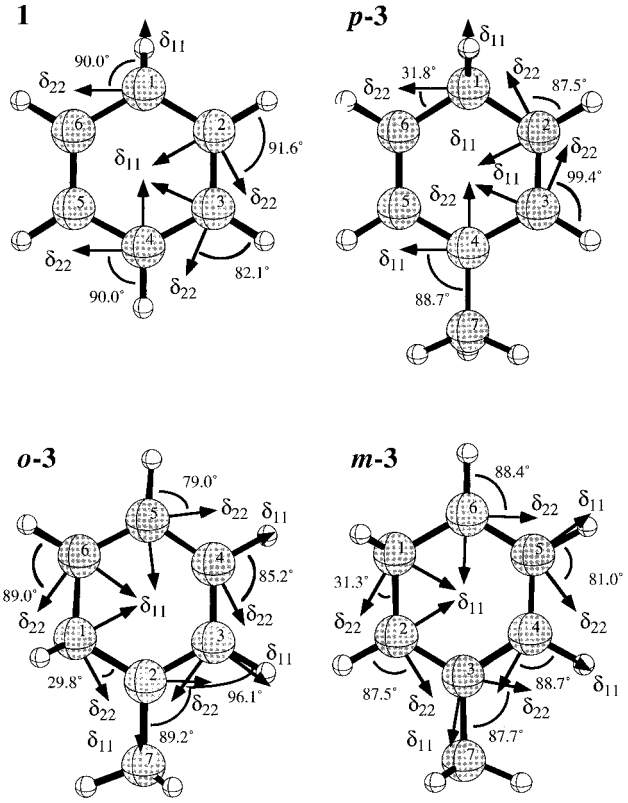

Figure 8. Orientations of the chemical shift tensors for ions **1**, *p*-**3**, *o*-**3**, and *m*-**3**. With the exception of C_3 and C_5 (see text) in *p*-**3**, in all shown cases δ_{11} and δ_{22} lie in the plane of the ring (the plane of the page), and δ_{33} lies perpendicular to that plane (out of the page).

Scheme 2

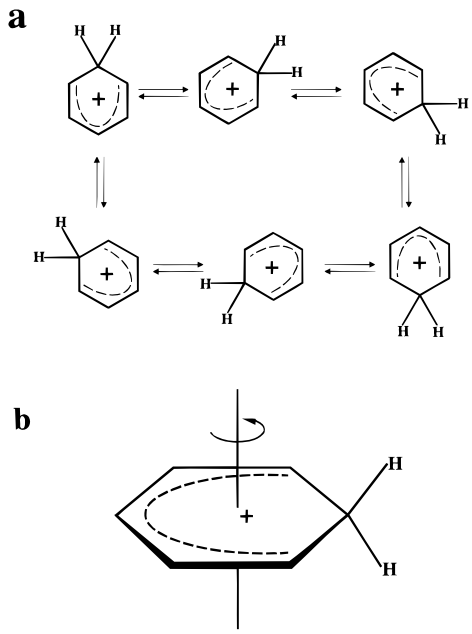

the normal, pointing toward C_7. Protonation in the *ortho* or *meta* positions also tilts some of the δ_{11} values slightly away from their C−H bond vectors.

We now attempt to evaluate the cause and significance of the deviations in the measured and computed principal component data. Such agreement for the individual components is necessarily worse than for the isotropic shift, as the latter is an average of the former. Furthermore, the magnitude of the errors can appear worse if the principal components are tabulated in terms of δ_{iso}, η, and CSA. δ_{iso} is known to a high degree of

accuracy, and the error from the principal components is concentrated in the asymmetry parameter and the anisotropy. Therefore, the experimental asymmetry parameters in Tables 2−5 are not in especially good agreement with the calculated values. We have also seen this disagreement in unpublished work in which the experimental measurements could be carried out with smaller confidence intervals.

Given the generally excellent agreement between the experimental and theoretical isotropic shifts, attempting to model the influence of the medium, as was necessary for the isopropyl[63] and *tert*-butyl cations,[64] is not warranted here. The only evidence to the contrary is that the inset in Figure 4d suggests that the isotropic shifts of benzenium ions undergoing isotropic vs anisotropic tumbling differ by 2 ppm.

The individual components are almost certainly more sensitive to deficiencies in basis sets or treatment of correlation than are the isotropic shifts. Our suspicion is that the greatest source of the discrepancy for the principal components measured and calculated here is the present state of theoretical methodology. At this point, however, we are satisfied with the level of agreement that we did obtain and the interplay between experiment and theory in treating dynamics of benzenium ions in the solid state.

Acknowledgment. This work was supported by the National Science Foundation (CHE-9528959) and U.S. Department of Energy (Grant No. DE-FG03-93ER14354). This work was partially supported by the National Center for Supercomputing Applications under Grant MCA96N010N and utilized the Silicon Graphics Power Challenge at the National Center for Supercomputing Applications, University of Illinois at Urbana-Champaign. We thank Dr. John B. Nicholas at Pacific Northwest National Laboratory for his comments on the manuscript. Computer resources were also provided by the Texas A&M University Supercomputing Facility.

JA963082T

(63) Nicholas, J. B.; Xu, T.; Barich, D. H.; Torres, P. D.; Haw, J. F. *J. Am. Chem. Soc.* **1996**, *118*, 4202−4203.

(64) Olsson, L.; Ottosson, C.; Cremer, D. *J. Am. Chem. Soc*. **1995**, *117*, 7460−7479.